J. Phys.: Condens. Matter **22** (2010) 055801 (10pp) doi:10.1088/0953-8984/22/5/055801

Theoretical calculation of the dislocation width and Peierls barrier and stress for semiconductor silicon*

Shaofeng Wang, Huili Zhang, Xiaozhi Wu and Ruiping Liu

Institute for Structure and Function, Chongqing University, Chongqing 400030, People's Republic of China

E-mail: sfwang@cqu.edu.cn

Received 23 September 2009, in final form 7 December 2009
Published 15 January 2010
Online at stacks.iop.org/JPhysCM/22/055801

Abstract

The dislocation width and Peierls barrier and stress have been calculated by the improved Peierls–Nabarro (PN) theory for silicon. In order to investigate the discreteness correction of a complex lattice quantitatively, a simple dynamics model has been used in which interaction attributed to a variation of bond length and angle has been considered. The results show that the dislocation core and mobility will be corrected significantly by the discrete effect. Another improvement is considering the contribution of strain energy in evaluating the dislocation energy. When a dislocation moves, both strain and misfit energies change periodically. Their amplitudes are of the same order, but phases are opposite. Because of the opposite phases, the misfit and strain energies cancel each other and the resulting Peierls barrier is much smaller than that given by the misfit energy conventionally. Due to competition between the misfit and strain energies, a metastable state appears separately for glide 90° and shuffle screw dislocations. In addition, from the total energy calculation it is found that besides the width of dislocation, the core of a free stable dislocation may be different according to where the core center is located. The exact position of the core center can be directly verified by numerical simulation, and provides a new prediction that can be used to verify the validity of PN theory. It is interesting that after considering discrete correction the Peierls stress for glide dislocation coincides with the critical stress at low temperature, and the Peierls stress for shuffle dislocation coincides with the critical stress at high temperature. The physical implication of the results is discussed.

1. Introduction

Silicon is an elemental covalent semiconductor crystallizing in the diamond structure. As a highly covalent crystal, silicon is hard to deform plastically at room temperature and is deformable only above several hundred degrees celsius [1–5]. The temperature dependence of the critical shear stress has a steep increase near 700 K [1–3] (873 K [6, 7]). It increases from 100 MPa to 1 GPa when the temperature decreases from 700 to 500 K [4, 8]. Such a steep change in the critical shear stress implies a transition from ductile to brittle. Dislocations are responsible for crystal plasticity and the critical shear stress is related to the mobility of the dislocations. Understanding of the structure and motion of dislocations is therefore crucial to obtain a comprehensive picture of silicon plasticity.

In silicon, predominant slip systems are the 60° and screw dislocations oriented along ⟨110⟩ directions in the {111} slip plane and the dislocations may be present in the glide or shuffle set configurations [9]. The dislocation is referred to as a shuffle one if the cut plane is between the widely spaced {111} planes, and a glide one if between the closely spaced {111} planes (see figure 1). Besides, the glide 60° and screw dislocations dissociate into a 30° and a 90° partial dislocation and into two 30° partial dislocations respectively, separated by a ribbon of intrinsic stacking fault [10–12]. There is no low energy stacking fault for a shuffle set, and so the shuffle dislocation does not dissociate. Because silicon is brittle at room temperature, it is difficult in experiment to obtain the Peierls stress, the stress required to move the

* The work is supported by the National Natural Science Foundation of China (Grant No. 10774196) and Chongqing University Postgraduates' Science and Innovation Fund (Grant No. 200904A1A0010315).

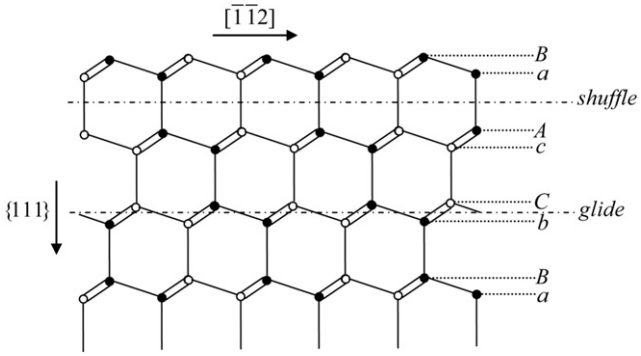

Figure 1. The glide set and shuffle set in silicon. When the lattice is divided by the cut plane given by the dashed line, for the glide set, as a repeat unit, the surface layer is composed of two planes with the same index (*Aa*, *Bb* or *Cc*), while for the shuffle set the surface layer is composed of two planes with different index (*Ac*, *Ba* or *Cb*). The atoms in the glide surface layer are connected through a vertical bond, but the atoms in the shuffle surface layer are connected through three nearly horizontal bonds. As a consequence, the discrete effect originating from the interaction between the atoms in the surface layer must be much larger for the shuffle set than for glide set.

dislocation from one lattice site to the next. The Peierls stress estimated by extrapolating the yield strengths to the absolute zero temperature is of the order $0.1\mu - 0.5\mu$ (7–34 GPa), where μ is the shear modulus [13–15]. Recently, a great deal of attention has been paid to the core reconstruction of dislocations in silicon [16–24]. It is believed that dislocation motion occurs by nucleation and propagation of kinks along the dislocation line. Due to thermal fluctuation or the action of an applied stress, double kinks can be nucleated and the individual kinks propagate in opposite directions. However, formation and migration of kinks are intimately related to the basic characteristics of dislocations in the ground state. Although dislocations in silicon have been studied extensively, understanding of the core structure and relevant features of dislocations in the ground state still need to be improved. For instance, there is a long-standing controversy: which dislocation moves more easily, glide or shuffle [25–29]? Initially, it is generally believed that in silicon the glide dislocation should move more easily than the shuffle dislocation [9]. The direct observation of the dissociated dislocation seems in favor of the glide set [30–33]. However, there is evidence that the Peierls stress of shuffle dislocation should be lower than that of glide dislocation [28, 34–37].

There are continuous efforts to improve the understanding of the relationship between dislocation properties and crystal characteristics. A number of numerical calculations have been carried out using atomistic simulation or an electron density functional technique, and a variety of results have been obtained [16–25, 38, 39]. Meanwhile, analytical PN theory, which is physically transparent, was used to investigate the basic properties of dislocations. In the classical PN model [9, 34, 40], the crystal with a dislocation is firstly cut into two parts and treated in a continuum framework. The dislocation is produced through nonlinear interaction between two parts and the interaction was taken to be sinusoidal with an amplitude determined by imposing the proper elastic slope. Later development recognized that a physically more realistic description of the restoring force is given by the generalized stacking fault energy surface (γ-surface) first suggested by Christian and Vitek [41]. Since the discrete effect is missed in the continuum approximation, the classical PN model becomes increasingly inaccurate for narrow dislocations [34, 35, 42]. Besides, the discrete effect will remarkably modify the core structure where the displacement field varies rapidly [43]. Recently, one of the authors had successfully relaxed the continuum approximation and obtained an improved PN equation based on the lattice dynamics [43–45]. The discrete effect is represented by a term proportional to the second-order derivative of displacement in the improved PN equation. Physically, the discrete term originates mainly from the interaction between the atoms on misfit planes. Even for the wide dislocations in simple metals, the agreement between the theoretical prediction and numerical simulation can be improved remarkably when the improved PN equation is applied [46, 47]. For the narrow dislocations in silicon, the discrete effect is no doubt more important and should be considered adequately.

In this paper, the core structures of dislocations in silicon have been studied by the improved PN equation which includes the correction from discreteness, and the Peierls barrier and stress have been evaluated by considering the contribution of strain energy. It is found that in addition to width the core of dislocations in silicon may exhibit distinct fine structure. Furthermore, the total energy calculation shows that there exists a metastable state for glide 90° or shuffle screw dislocations. Our theoretical predictions can be verified directly by numerical simulation. The Peierls stress obtained in our calculation is about 10 GPa for a glide dislocation, which coincides with the critical stress at low temperature. The Peierls stress of shuffle dislocation is greatly lowered by the discrete effect. It is smaller than 1 GPa which coincides with the critical stress at high temperature. Our results hint that glide dislocation may be responsible for the low temperature plasticity while shuffle dislocation is responsible for high temperature plasticity. It seems that at low temperature shuffle dislocation is absent and it appears when temperature is high enough. The transition from brittle to ductile is probably related to the excitation of shuffle dislocations. The outline of this paper is as follows. In section 2, the dislocation equation and γ-surface are discussed. Section 3 is focused on the correction of the discrete effect. In section 4, dislocation width and Peierls barrier and stress are calculated in detail. Section 5 is a discussion and summary.

2. Dislocation equation with correction from the lattice effect

The two-dimensional dislocation equation for straight dislocations can be obtained from the lattice dynamics and symmetry principle [45]

$$-\frac{\beta_e}{2}\frac{d^2u^x}{dx^2} - \frac{K_e\sigma}{2\pi}\int_{-\infty}^{+\infty}\frac{dx'}{x'-x}\left(\frac{du^x}{dx}\right)\Big|_{x=x'} = f_x, \quad (1)$$

Table 1. The γ_{us} in [34] and [27] and dimensionless parameters Δ_1 and Δ_2, where N, A and AV represent γ_{us} calculated with no relaxation, atomic relaxation at ideal volume and atomic and volume relaxation, respectively.

		Reference [34]		Reference [27]	
Glide set	γ_{us} (eV Å^{-2})	0.118 (AV)	0.157 (N)	0.126 (A)	0.119 (AV)
	Δ_1	−0.08	0.23	−0.01	−0.06
	Δ_2	0.00	0.00	0.00	0.00
Shuffle set	γ_{us} (eV Å^{-2})	0.105 (AV)	0.115 (N)	0.113 (A)	0.104 (AV)
	Δ_1	−0.80	−0.80	−0.80	−0.80
	Δ_2	0.63	0.71	0.70	0.63

$$-\frac{\beta_s}{2}\frac{d^2u^y}{dx^2}-\frac{K_s\sigma}{2\pi}\int_{-\infty}^{+\infty}\frac{dx'}{x'-x}\left(\frac{du^y}{dx}\right)\Bigg|_{x=x'}=f_y, \quad (2)$$

where K_e and K_s are the energy factors of the edge and screw dislocations [9], σ is the area of primitive cell of the misfit plane (which is a two-dimensional triangular lattice), u^x and u^y are the edge and screw components of relative displacement field, the coordinates axes x and y are, respectively, perpendicular and parallel to the dislocation line. The energy factors can be expressed in terms of effective elastic constants $K_e = \mu'/(1-\nu')$ and $K_s = \mu'$, with the values $\mu' = 63.75$ GPa and $\nu' = 0.256$ [9, 34]. The nonlinear interaction, $\mathbf{f} = (f_x, f_y)$, is given by the gradient of the γ-surface as suggested by Christian and Vitek

$$\mathbf{f} = -\nabla\gamma(\mathbf{u})\sigma.$$

Although the new equation is formally universal, the parameters β_e and β_s related to the discreteness correction depend on lattice structure and dislocation type. They will be given explicitly in section 3.

Following the method given in [34] and [47], equations (1) and (2) can be incorporated into a single equation for an arbitrary mixed dislocation

$$-\frac{\beta_b}{2}\frac{d^2u}{dx^2}-\frac{K_b\sigma}{2\pi}\int_{-\infty}^{+\infty}\frac{dx'}{x'-x}\left(\frac{du}{dx}\right)\Bigg|_{x=x'}=f_b(u), \quad (3)$$

with

$$\beta_b = \beta_e\sin^2\theta+\beta_s\cos^2\theta,$$
$$K_b = \mu'\left(\frac{\sin^2\theta}{1-\nu'}+\cos^2\theta\right), \quad (4)$$

where θ is the angle between dislocation line and Burgers vector, both u and $f_b(u)$ are defined along the Burgers vector. The γ-surfaces of silicon have been calculated by several groups [27, 34]. It is noted that the γ-surface along the ⟨112⟩ direction of the glide set and along the ⟨110⟩ direction of the shuffle set can be approximately expressed as

$$\gamma_b(u) = \frac{\mu' b^2}{4\pi^2 d}\left(1+\cos\frac{2\pi u}{b}\right)\times\left(1+\Delta_1\cos^2\frac{\pi u}{b}+\Delta_2\cos^4\frac{\pi u}{b}\right), \quad (5)$$

where the sum $\Delta = \Delta_1 + \Delta_2$ is given by the unstable stacking fault energy $\gamma_{us} = \mu' b^2(1+\Delta)/2\pi^2 d$.

In table 1, γ_{us}, Δ_1 and Δ_2 are listed for fitting the γ-surface given in [34] and [27]. In figure 2, the γ-surface along the ⟨112⟩ direction of the glide set and along the ⟨110⟩ direction of the shuffle set given by Joos *et al* [34] and by equation (5) are plotted. Apart from the intrinsic stacking fault energy which is small for silicon, fitting is satisfactory.

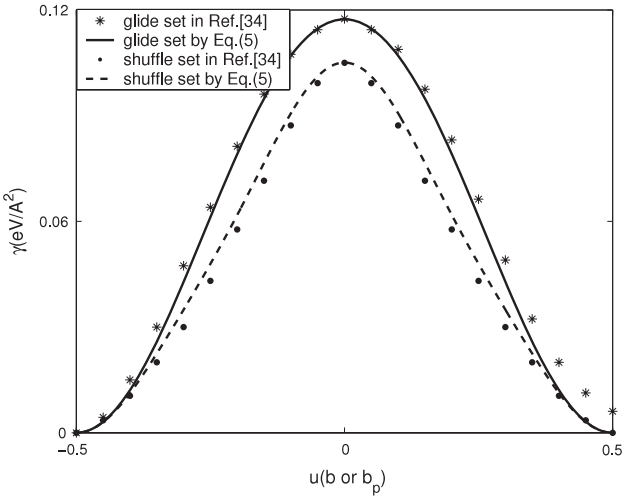

Figure 2. The γ-surface along the ⟨112⟩ direction (the upper one) and along the ⟨110⟩ direction (the lower one) given by Joos *et al* [34] and by equation (5), where $b_p = 2.22$ Å is the Burgers vector of glide partials, and $b = 3.84$ Å is the Burgers vector of shuffle dislocations. Apparently, the numerical results can be well described by equation (5).

The γ-surface has a great effect upon the dislocation characteristics. As recovery of the elastic limit is required for small deformation, the most important factor is the unstable stacking fault energy γ_{us} that measures the height of a γ-surface. In comparing with the shuffle set, the γ_{us} of the glide set more sensitively depends on whether relaxation is allowed and how it occurs. Because of bond flip appearing for large distortion, the relaxed γ-surface should be more suitable than the unrelaxed one. The unstable stacking fault energy γ_{us} of the glide set is larger than that of the shuffle set, as a consequence, it is expected that the width of the shuffle dislocation should be wider than that of the glide dislocation.

3. Evaluation of parameters β_e and β_s by using a dynamic model

As pointed out in [44, 45], the second-differential terms newly appeared in the dislocation equations represent the lattice discrete effect. They mainly result from the surface effect.

When a crystal is viewed as a set of parallel lattice planes, the surface plane is not equivalent to those in the interior. As is well known, the misfit planes become the surface planes of the semi-crystals while the crystal is cut into two semi-crystals for constructing a dislocation. In the continuum approximation, the distinction between the surface and internal planes cannot be recognized and the surface effect is missed. From exactly solvable models [43, 44] in which discreteness of a lattice can be fully considered, one clearly sees the discreteness correction appearing in terms of the second-differential of the displacement. Physically, the integro term in the dislocation equation represents a long range interaction which is inversely proportional to the distance, the differential term describes short range interaction which results from the interaction among the atoms on the surface plane.

The discrete parameters β_e and β_s are, respectively, related to the longitudinal and transverse wave velocities (c_{sl} and c_{st}) of the surface that is decoupled [45]

$$\beta_e = \tfrac{1}{2}\rho_s \sigma c_{sl}^2, \tag{6}$$

$$\beta_s = \tfrac{1}{2}\rho_s \sigma c_{st}^2. \tag{7}$$

For Bravais lattices, acoustic wave velocities c_{sl} and c_{st} can be approximately given by the structural and elastic constants. However, the results for Bravais lattices are no longer valid for complex lattices. In silicon, there are two kinds of dislocations with the same Burgers vector: glide and shuffle dislocations. As shown in figure 1, when the lattice is divided by the cut plane, the surface layer as a repeat unit is composed of planes with the same index (Aa, Bb or Cc) for glide dislocation, and is composed of planes with different index (Ac, Ba or Cb) for shuffle dislocation. The surface layers are so different for glide and shuffle dislocations that the relevant discrete parameters are different and should be treated separately.

In order to investigate the discrete parameters β_e and β_s quantitatively, a simple dynamics model is used to explore the relationship between the parameters and silicon characteristics. The lattice Hamiltonian includes the interaction energy attributed to variation of bond length and angle

$$\begin{aligned} H = \frac{1}{2}\sum_{\mathbf{R}} \Bigg\{ \Bigg[& \frac{\alpha_1}{2|\mathbf{b}_i|^2} \sum_{i=1}^{4} (\nabla_{\mathbf{b}_i} \mathbf{u}_\mathbf{R} \cdot \mathbf{b}_i)^2 \\ & + \frac{\alpha_2}{2|\mathbf{b}_i|^2} \sum_{j=1}^{3} \sum_{k>j} (\nabla_{\mathbf{b}_j} \mathbf{u}_\mathbf{R} \cdot \mathbf{b}_k + \nabla_{\mathbf{b}_k} \mathbf{u}_\mathbf{R} \cdot \mathbf{b}_j)^2 \Bigg] \\ & + \Bigg[\frac{\alpha_1}{2|\mathbf{b}_i|^2} \sum_{i=1}^{4} (\nabla_{-\mathbf{b}_i} \mathbf{v}_\mathbf{R} \cdot \mathbf{b}_i)^2 + \frac{\alpha_2}{2|\mathbf{b}_i|^2} \\ & \times \sum_{j=1}^{3} \sum_{k>j} (\nabla_{-\mathbf{b}_j} \mathbf{v}_\mathbf{R} \cdot \mathbf{b}_k + \nabla_{-\mathbf{b}_k} \mathbf{v}_\mathbf{R} \cdot \mathbf{b}_j)^2 \Bigg] \Bigg\}, \end{aligned} \tag{8}$$

with

$$\nabla_{\mathbf{b}_i} \mathbf{u}_\mathbf{R} = \mathbf{v}_{\mathbf{R}+\mathbf{b}_i} - \mathbf{u}_\mathbf{R}, \qquad \nabla_{-\mathbf{b}_i} \mathbf{v}_\mathbf{R} = \mathbf{u}_{\mathbf{R}-\mathbf{b}_i} - \mathbf{v}_\mathbf{R}, \tag{9}$$

where α_1 and α_2 are force constants describing the force produced by variation of bond length and angle, $\mathbf{u}_\mathbf{R}$ and $\mathbf{v}_\mathbf{R}$ the displacements of the two atoms in the same primitive cell,

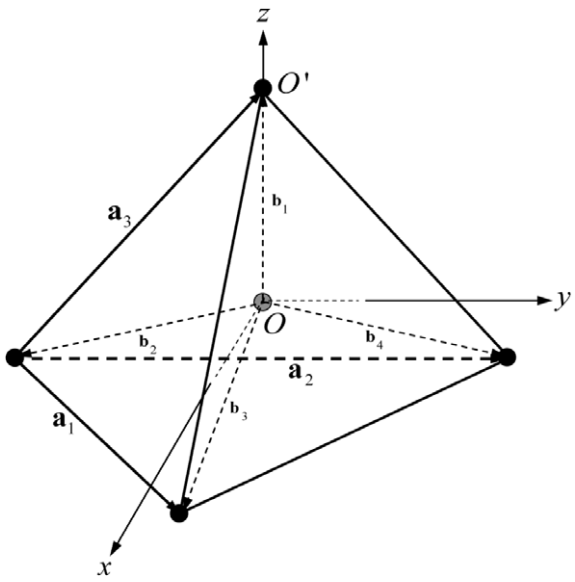

Figure 3. The basis vectors $\mathbf{a}_i$ ($i = 1, 2, 3$) and bond vectors $\mathbf{b}_i$ ($i = 1, 2, 3, 4$) of silicon. For an atom (at point O) in the diamond lattice, there are four nearest neighbor atoms forming a regular tetrahedron, bond vectors $\mathbf{b}_i$ connect the atom to its nearest neighbors. The horizontal closest-packed plane is chosen to be the x–y plane, where y is along the closest-packed line. The displacements of atoms at points O and O′ are, respectively, denoted by $\mathbf{v}_\mathbf{R}$ and $\mathbf{u}_\mathbf{R}$.

$\mathbf{a}_i$ ($i = 1, 2, 3$) are the basis vectors and $\mathbf{b}_i$ ($i = 1, 2, 3, 4$) the bond vectors (see figure 3).

At first, one needs to determine the interaction constants and verify the validity of the model. It can be proved that under homogeneous deformation, the energy density is given by

$$\begin{aligned} \varepsilon = & \frac{\alpha_1 + 6\alpha_2}{6a_0}(e_1^2 + e_2^2 + e_3^2) \\ & + \frac{2(\alpha_1 - 2\alpha_2)}{6a_0}(e_1e_2 + e_1e_3 + e_2e_3) \\ & + \frac{16\alpha_1\alpha_2}{3(\alpha_1 + 2\alpha_2)a_0}(e_4^2 + e_5^2 + e_6^2). \end{aligned} \tag{10}$$

Thus

$$c_{11} = \frac{\alpha_1 + 6\alpha_2}{3a_0}, \qquad c_{12} = \frac{\alpha_1 - 2\alpha_2}{3a_0},$$
$$c_{44} = \frac{8\alpha_1\alpha_2}{3a_0(\alpha_1 + 2\alpha_2)},$$

where $a_0 = 5.43$ Å is the lattice constant. We select c_{11} and c_{12} to determine force constants

$$\alpha_1 = \frac{3a_0(c_{11} + 3c_{12})}{4}, \qquad \alpha_2 = \frac{3a_0(c_{11} - c_{12})}{8} \tag{11}$$

and then calculate c_{44} as predicted from the model. The results are listed in table 2. One sees that the c_{44} given by the model are in accordance with experimental data.

Now, we need to decouple the surface layer, i.e. cancel the interaction between the surface layer and interior layers. To do this, the interaction force is firstly expressed in terms of relative displacements of paired atoms and each individual term is interpreted as an interaction between the paired atoms. We then

Table 2. The atomic force constants α_1 and α_2 calculated from equation (11) using the elastic constants c_{11} and c_{12} in [48–50] and c_{44} calculated from equations (11). Also shown are the elastic constants obtained through continuum elasticity theory by Jakata and Every [48], medium of the shell model (SM), molecular dynamics (MD) and *ab initio* lattice dynamics (Ab) by Maranganti and Sharma [49] and Landolt-Bornstein [50]. The elastic constants are in units of 10^2 GPa and force constants in units of 10^2 N m^{-1}.

	Reference [48]	Reference [49] (MD)	Reference [49] (Ab)	Reference [49] (SM)	Reference [50]
c_{11}	1.78	1.45	1.68	1.66	1.65
c_{12}	0.75	0.84	0.45	0.48	0.63
c_{44}	0.81	0.70	0.81	0.80	0.79
α_1	1.63	1.62	1.23	1.26	1.44
α_2	0.21	0.12	0.25	0.24	0.21
c_{44} (by model)	0.82	0.53	0.87	0.85	0.79

only keep the terms that represent the interaction between the atoms in the surface layer. Because only the plane deformation is of interest, the normal displacement is fixed to be zero. The next step is adding the forces felt by the atoms in a cell and obtaining the relation between the total force acting on the cell and the displacement. The last step is taking the continuum approximation and obtaining the acoustic wave velocity of the surface layer. In such a way, the discrete parameters can be expressed by the force constants. For the case of the glide set, one has $\mathbf{u_R} = \mathbf{v_R}$ because the surface layer is composed of two face-to-face triangle lattices and only long-wavelength acoustic waves are considered. The relationship between the interaction force and displacement is

$$\begin{pmatrix} f_{\mathbf{R}}^x \\ f_{\mathbf{R}}^y \end{pmatrix} = \begin{pmatrix} \frac{2\alpha_2}{9}(2\Delta_1 + 2\Delta_{12} - \Delta_2) & \frac{2\alpha_2}{3\sqrt{3}}(\Delta_1 - \Delta_{12}) \\ \frac{2\alpha_2}{3\sqrt{3}}(\Delta_1 - \Delta_{12}) & \frac{2\alpha_2}{3}\Delta_2 \end{pmatrix} \times \begin{pmatrix} u_{\mathbf{R}}^x \\ u_{\mathbf{R}}^y \end{pmatrix}, \tag{12}$$

with

$$\Delta_1 = T_1 + T_1^{-1} - 2, \qquad \Delta_2 = T_2 + T_2^{-1} - 2,$$

$$\Delta_{12} = T_1 T_2^{-1} + T_1^{-1} T_2 - 2,$$

where $\mathbf{T}_i$ $(i = 1, 2)$ are the translation operators, $\mathbf{T}_i \mathbf{u_R} = \mathbf{u_{R+a}}_i$. In the slowly varying approximation, equation (12) becomes

$$\begin{pmatrix} f_{\mathbf{R}}^x \\ f_{\mathbf{R}}^y \end{pmatrix} = \begin{pmatrix} \frac{2\alpha_2 a^2}{3}\frac{\mathrm{d}^2}{\mathrm{d}x^2} & \frac{\alpha_2 a^2}{3}\frac{\mathrm{d}^2}{\mathrm{d}x\,\mathrm{d}y} \\ \frac{\alpha_2 a^2}{3}\frac{\mathrm{d}^2}{\mathrm{d}x\,\mathrm{d}y} & \frac{2\alpha_2 a^2}{3}\frac{\mathrm{d}^2}{\mathrm{d}y^2} \end{pmatrix} \begin{pmatrix} u_{\mathbf{R}}^x \\ u_{\mathbf{R}}^y \end{pmatrix}, \tag{13}$$

where $a = a_0/\sqrt{2}$ is the length of the primitive vector (period in the direction of the dislocation line). From equations (6), (7) and (13), it is easy to obtain

$$\beta_e = \frac{\alpha_2 a^2}{3} = \frac{(c_{11} - c_{12})a_0^3}{16}, \qquad \beta_s = 0. \tag{14}$$

In a similar way, the parameters β_e and β_s can be obtained for the case of the shuffle set

$$\beta_e = \frac{2(\alpha_1 + \alpha_2)a^2}{9}, \qquad \beta_s = \frac{\alpha_2 a^2}{3},$$

or in terms of elastic constants

$$\beta_e = \frac{(3c_{11} + 5c_{12})a_0^3}{24}, \qquad \beta_s = \frac{(c_{11} - c_{12})a_0^3}{16}.$$

The parameters β_e and β_s that describe the discrete effect depend on the structure detail as well as the elastic constants. When a complex lattice is dealt with, these parameters may be quite different for different dislocations even though their Burgers vectors are the same. Our evaluation presents an approximated method to extract the parameters β_e and β_s from the long-wavelength dynamics of the crystal. A simple way to obtain the parameters is by investigating the tensile deformation perpendicular to the dislocation line and the shear deformation along the dislocation line and finding the relation between the force and displacement. Actually, the parameters β_e and β_s are, respectively, the effective tensile and shear constants.

4. Dislocation width and Peierls barrier and stress

The dislocation equation is a nonlinear integro-differential equation and can be hardly solved exactly. The dislocation solution of the classical Peierls equation was usually obtained through a rational superposition of small dislocations [34, 36, 51, 52]. Recently, a new method, the truncating method for solving the dislocation equation, was proposed by Wang [53]. The trial solution only has one constant that needs to be determined

$$u = \frac{\mathrm{b}}{\pi}\left(\arctan q + \frac{cq}{1+q^2}\right), \tag{15}$$

with

$$q = kx, \qquad k = k_0(1 - c),$$
$$k_0 = \frac{2}{d}\left(\frac{\sin^2\theta}{1-\nu'} + \cos^2\theta\right)^{-1}, \tag{16}$$

where b is the Burgers vector, d is the spacing between glide planes and c is a constant determined by the dislocation equation. For convenience, we have listed the elementary constants in table 3.

The dislocation density is given by

$$\frac{\mathrm{d}u}{\mathrm{d}x} = \frac{kb}{\pi}\left[\frac{1-c}{1+q^2} + \frac{2c}{(1+q^2)^2}\right], \tag{17}$$

which is a kind of power series that converges rapidly. Noting that far from the dislocation core, dislocation density is independent of parameter c

$$\frac{\mathrm{d}u}{\mathrm{d}x} = \frac{b}{k_0 \pi x^2},$$

Table 3. The elementary constants: Burgers vector b, spacing d, parameters k_0 and β_b and energy factor K_b for various dislocations, where elastic constants in [50] are used.

Dislocation	b (Å)	d (Å)	k_0 (Å^{-1})	β_b (eV)	K_b (eV Å^{-3})
Glide 30°	2.22	0.78	2.35	1.60	0.43
Glide 90°	2.22	0.78	1.90	6.40	0.54
Shuffle 60°	3.84	2.35	0.68	26.93	0.50
Shuffle screw	3.84	2.35	0.85	6.38	0.40

the asymptotic behavior of the dislocation is therefore controlled by k_0, which only depends on the elasticity of the crystal. Parameter c only has an effect on the core structure and can be referred to as the core parameter of a dislocation. Substituting the solution of equation (15) into equation (3) and following the truncating method [53], it is found that c should satisfy the algebraic equation

$$\frac{2\beta_b\mu'}{K_b^2\sigma d}(1+2c)(1-c)^2-\frac{4c^2}{5}-\Delta_1\left(1+\frac{c}{5}\right)-\frac{6\Delta_2}{5}=0. \quad (18)$$

The first term proportional to β_b represents the correction from the discrete effect. If parameters β_b, Δ_1 and Δ_2 vanish, then $c = 0$ and equation (15) is just the exact solution of the classical PN equation. If parameter β_b equals zero, one recovers the classical PN model with a generalized stacking fault restoring force. The core parameters c calculated from equation (18) and half width ξ, defined as the distance over which u changes from 0 to $b/4$ are listed in table 4.

It is shown that the half width obtained by the truncating method agrees well with the result (in parenthesis) given by Joos *et al* when the discrete effect is not considered. This suggests that the truncating method is efficient and convenient since there is only one constant that needs to be determined and the results are satisfactory. After considering the correction from the discrete effect, the half width of the dislocation becomes wider, but the correction is very different for different dislocations (see table 4). For shuffle 60° dislocation, the correction is especially large and the width is doubled (1.61 Å changes to 3.57 Å). For the 30° partial dislocation, the correction is relatively small and the width is still very narrow (0.64 Å). Although the discrete parameter β_b is nearly the same for a 90° partial dislocation and shuffle screw dislocation, correction to the 90° partial dislocation is larger because it is narrower. The narrower the dislocation is, the more the correction by the discrete effect.

In the classical PN theory, the Peierls barrier and stress are obtained by calculating the misfit energy associated with discreteness of the lattice. However, it has been shown that the contribution from the strain energy may be larger than that from the misfit energy [54]. The total energy including the contribution from both misfit and strain energies should be evaluated to obtain the correct result. In PN theory, the Hamiltonian can be written as a sum of three terms

$$H = H_a + H_b + H_{ab},$$

where H_a (H_b) is the Hamiltonian of the semi-crystal above (below) the cut plane, H_{ab} is the interaction between two

Table 4. The core parameter c and half width ξ calculated by considering discrete effect. c_0 and ξ_0 are the results given by the classical PN model with the same γ-surface. The width is given in units of the Burgers vector b. For comparison, the results in [34] are also shown in parenthesis.

Dislocation	Δ_1	Δ_2	c_0	c	ξ_0 (b)	ξ (b)
30°	−0.08	0.00	0.33	0.62	0.21(0.21)	0.29
partials	0.23	0.00	—	0.44	—	0.23
	−0.01	0.00	0.11	0.58	0.19	0.27
	−0.06	0.00	0.28	0.61	0.20	0.28
90°	−0.08	0.00	0.33	0.72	0.26(0.26)	0.45
partials	0.23	0.00	—	0.62	—	0.36
	−0.01	0.00	0.11	0.70	0.24	0.43
	−0.06	0.00	0.28	0.72	0.25	0.45
Shuffle 60°	−0.80	0.63	0.35	0.79	0.42(0.51)	0.93
	−0.80	0.71	—	0.76	—	0.83
	−0.80	0.70	—	0.77	—	0.86
Shuffle screw	−0.80	0.63	0.35	0.70	0.34(0.41)	0.55
	−0.80	0.71	—	0.66	—	0.50
	−0.80	0.70	—	0.66	—	0.50

semi-crystals divided by the cut plane. Each semi-crystal is approximated as a harmonic one in which atoms interact through a harmonic force. The potential energy due to deformation of the semi-crystals is referred to as strain energy while the interaction energy is referred to as misfit energy. It was proved that in equilibrium the potential energy of a harmonic semi-crystal imposed by external force $\mathbf{f}$ can be obtained by [54]

$$H_a = \tfrac{1}{2}\sum_i \mathbf{f}_i \cdot \mathbf{u}_i,$$

where the sum runs over the atoms on which the nonzero external force is imposed. Therefore, for a dislocation with length L, the strain and misfit energies of dislocation per unit length are given by

$$E_s(x_0) = \frac{1}{L}(H_a + H_b) = \frac{1}{2}\sum_{l=-\infty}^{\infty} f_b(u_l)u_l \times \frac{\sigma}{a}, \quad (19)$$

$$E_m(x_0) = \frac{H_{ab}}{L} = \sum_{l=-\infty}^{\infty} \gamma_b(u_l) \times \frac{\sigma}{a}, \quad (20)$$

where $u_l = u(x_l - x_0)$ is the relative displacement for dislocation located at x_0, a is the length of the primitive vector (period in the direction of the dislocation line) and the sum is carried over the atoms in the horizontal band with width a in a misfit plane (figure 4). The dislocation energy per unit length is

$$E_{dis}(x_0) = E_s(x_0) + E_m(x_0). \quad (21)$$

Substituting the γ-surface and the resulting force into the above equations, we have

$$\begin{aligned} E_{dis} = \sum_{l=-\infty}^{\infty} \frac{\mu' b^2\sigma}{4\pi^2 ad}\Bigg\{ & \left(1+\cos\frac{2\pi u_l}{b}\right) \\ & \times \left(1+\Delta_1\cos^2\frac{\pi u_l}{b}+\Delta_2\cos^4\frac{\pi u_l}{b}\right) \\ & + \Bigg[(1+\Delta_1)\sin\frac{2\pi u_l}{b}+\frac{\Delta_1}{2}\sin\frac{4\pi u_l}{b} \\ & + 3\Delta_2\sin\frac{2\pi u_l}{b}\cos^4\frac{\pi u_l}{b}\Bigg]u_l\Bigg\}. \end{aligned} \quad (22)$$

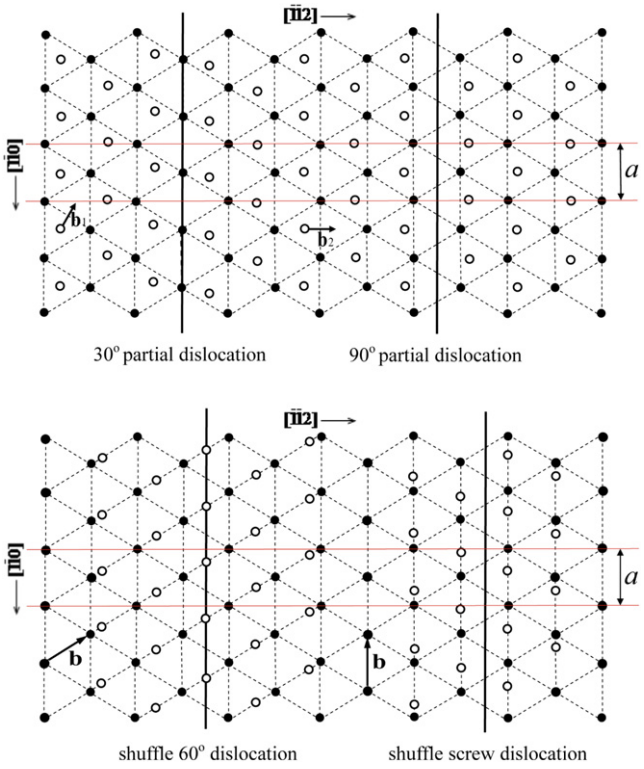

Figure 4. Core structure of dislocations. The solid and empty circles, respectively, represent the atoms on the misfit planes that are below and above the cut plane. For simplicity, the distortion is shown by the relative displacements of atoms on the upper misfit plane. In addition to the width of dislocations, the core structures are distinct. The symmetry axis plotted by a solid line can be located at the middle of two atom rows (90° partial dislocation and shuffle screw dislocation) or coincide with one atom row (30° partial dislocation and shuffle 60° dislocation).

For a narrow dislocation like the one in silicon, the series in the summation converges rapidly apart from an additional constant that has no contribution to the Peierls barrier and Peierls stress [35]. From the total energy calculation, it is found that besides the width of the dislocation, the dislocation core of a free stable dislocation may be different according to where the symmetry axis (solid line in figure 4) is located. For the glide 90° dislocation and shuffle screw dislocation, the symmetry axis is located at the middle of two atom rows and no atom appears on the symmetry axis. For the glide 30° dislocation and shuffle 60° dislocation, the symmetry axis coincides with an atom row of one misfit plane and so atoms appear on the axis. In addition, for a glide 30° dislocation, the atoms on the misfit plane, in which the symmetry axis coincides with an atom row, have a tendency to accumulate toward the core center. In contrast, for a shuffle 60° dislocation, the atoms on the plane have a tendency to disperse outward. Therefore, just from the atom configuration at the core center, one can recognize three types of dislocations. The exact position of the core center can be directly verified by numerical simulation, and it provides a new prediction that can be used to verify the validity of PN theory.

As a function of dislocation position, the misfit energy, strain energy and total energy have been calculated and plotted in figure 5, and the Peierls barriers for various dislocations are shown in table 5. The results clearly tell us that when a dislocation moves, both strain and misfit energies change periodically. Their amplitudes are of the same order, but phases are opposite. The amplitude of the misfit energy is larger than that of the strain energy for the glide dislocations and shuffle screw dislocation. In contrast, for the shuffle 60° dislocation the amplitude of the misfit energy is smaller. Because of opposite phases, the misfit and strain energies cancel each other and the Peierls barrier is much smaller than that conventionally given by the misfit energy. In particular, for the glide 90° partial and shuffle screw dislocations, the amplitudes of misfit and strain energies are nearly equal and cancelation occurs. The Peierls barrier is nearly one order of magnitude lower. Therefore, it is necessary to consider the strain energy as well as misfit energy. Besides, due to competition between the misfit and strain energies, a small energy valley appears between two neighbor ground state positions for the glide 90° and shuffle screw dislocations. In particular, for the glide 90° dislocation, the valley depth is nearly a half of the barrier height. The new energy valley implies that there is a metastable state aside from the ground state. It is observed that the appearance of the metastable state is closely related to where the symmetry axis lie; it appears only when the axis lies between two atom rows.

Table 5. The Peierls barriers in units of 10^{-2} eV Å^{-1} for various dislocations. E_p is obtained from the total energy, $E_p^m(0)$ and E_p^m are obtained from the misfit energy only, $E_p^m(0)$ does not take into consideration the correction from the discrete effect. For comparison, the results in [34] are also shown in parenthesis.

Dislocation	Δ_1	Δ_2	$E_p^m(0)$	E_p^m	E_p
30°	−0.08	0.00	35 (34.3)	33	12
partials	0.23	0.00	—	47	28
	−0.01	0.00	38	36	16
	−0.06	0.00	36	34	13
90°	−0.08	0.00	33 (32.3)	23	1.6
partials	0.23	0.00	—	41	17
	−0.01	0.00	36	28	4.3
	−0.06	0.00	33	24	2.0
Shuffle 60°	−0.80	0.63	13 (11.6)	1.3	1.8
	−0.80	0.71	—	2.7	2.8
	−0.80	0.70	—	2.2	2.6
Shuffle screw	−0.80	0.63	17 (14.8)	7.6	0.85
	−0.80	0.71	—	11	2.4
	−0.80	0.70	—	11	2.3

Due to discreteness of the lattice, a dislocation cannot move unless the applied stress exceeds the Peierls stress. The Peierls stress is the minimum stress needed to move a dislocation and it can be obtained from the maximum slope of the dislocation energy [9]

$$\sigma_p = \max \left| \frac{1}{b} \frac{\mathrm{d}E_{\mathrm{dis}}(x)}{\mathrm{d}x} \right|, \tag{23}$$

where both the misfit energy and the strain energy are considered. The Peierls stresses have been calculated and the results are listed in table 6. In order to verify our method used here, Peierls stresses $\sigma_p^m(0)$ given in the classical PN theory,

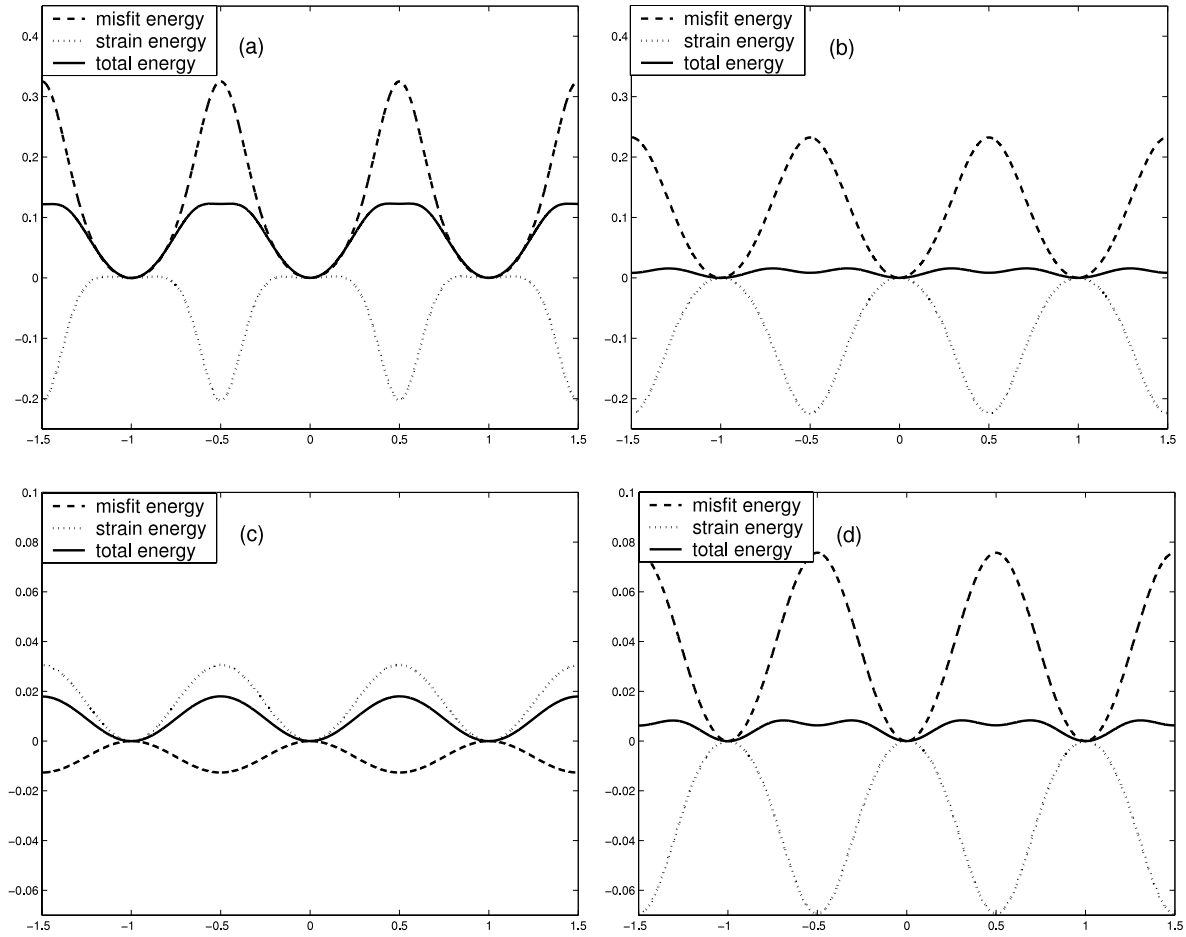

Figure 5. The misfit, strain and total energies as a function of dislocation position, where the x axis is in units of the period $\sqrt{3}a/2$, and the y axis in units of eV Å^{-1}. The energies are calculated by keeping the 20 and 50 leading terms in the summations, respectively, for the glide and shuffle dislocations. The ground energy is taken to be zero-point. There is a metastable state resulting from strong cancelation between the strain and misfit energies for 90° and screw dislocations. (a) Glide 30° partial; (b) glide 90° partial; (c) shuffle 60°; (d) shuffle screw.

Table 6. The Peierls stress in units of 10^{-2} eV Å^{-3} for various dislocations. $\sigma_{\rm p}$ is obtained from the total energy, $\sigma_{\rm p}^{\rm m}(0)$ and $\sigma_{\rm p}^{\rm m}$ are obtained from the misfit energy only, $\sigma_{\rm p}^{\rm m}(0)$ does not consider the correction from the discrete effect. For comparison, the results in [34] are also shown in parenthesis.

Dislocation	Δ_1	Δ_2	$\sigma_{\rm p}^{\rm m}(0)$	$\sigma_{\rm p}^{\rm m}$	$\sigma_{\rm p}$
30°	−0.08	0.00	24 (22)	17	6.5
partials	0.23	0.00	—	33	16
	−0.01	0.00	28	21	8.5
	−0.06	0.00	25	18	7.0
90°	−0.08	0.00	19 (18)	10	1.2
partials	0.23	0.00	—	21	8.6
	−0.01	0.00	23	12	2.6
	−0.06	0.00	20	11	1.4
Shuffle 60°	−0.80	0.63	3.3 (3.0)	0.31	0.44
	−0.80	0.71	—	0.66	0.69
	−0.80	0.70	—	0.55	0.63
Shuffle screw	−0.80	0.63	4.6 (4.1)	1.9	0.34
	−0.80	0.71	—	2.8	0.84
	−0.80	0.70	—	2.8	0.83

where only the misfit energy is considered and the discrete effect is neglected, are also listed for various dislocations. Our results are in good agreement with those obtained by Joos *et al* (given in parenthesis). If only the misfit energy is considered, the Peierls stress will be decreased by the discrete effect. This is not surprising because the discrete effect always makes the dislocations become wider. When the strain energy is also considered at the same time, the Peierls stress obtained from total energy is further decreased except for the case of a shuffle 60° dislocation. For a shuffle 60° dislocation, the amplitude of strain energy is much larger than that of misfit energy. As a result, the Peierls barrier and stress increase rather than decrease as for the other cases.

Apparently, the Peierls stresses predicted here are much smaller than those given by classical PN theory especially for shuffle dislocations. For the shuffle 60° dislocation, numerical results obtained by molecular dynamics or density functional theory are in the range between 0.4×10^{-2} and 1.7×10^{-2} eV Å^{-3} (0.6–2.8 GPa) [55–57]. Our result agrees well with the numerical one. For the shuffle screw dislocation, numerical results are in the range between 1.9×10^{-2} and 2.8×10^{-2} eV Å^{-3} (3–4 GPa) [58–60]. Our result obtained from the total energy calculation is smaller than the numerical one. It is noted that if only the misfit energy is considered, the resulting Peierls stresses are coincident for both the shuffle 60° and screw dislocation. For the glide 30° and 90° partials, the

atomic model gave 0.132 eV Å^{-3} (21 GPa) and 0.106 eV Å^{-3} (17 GPa) respectively [28].

It is interesting that the Peierls stress for the glide 30° dislocation is 0.065–0.16 eV Å^{-3} (10–26 GPa), which coincides with the critical stress at low temperature 0.043–0.215 eV Å^{-3} (6.9–34 GPa) extrapolated from experimental data [8, 13–15]. The Peierls stress for a shuffle dislocation is 3.4–8.4 meV Å^{-3} (0.54–1.3 GPa) which coincides with the critical stress at high temperature (∼1 GPa) observed in experiments [4, 8]. Our results strongly hint that glide dislocation may be responsible for the low temperature plasticity while shuffle dislocation may be responsible for high temperature plasticity. It seems that at low temperature shuffle dislocation is absent and it appears when temperature is high enough. The transition from brittle to ductile is probably related to excitation of shuffle dislocations.

5. Summary and discussion

The discrete effect that resulted from the interaction among the atoms on the misfit plane has been investigated theoretically for dislocations in silicon. The picture of dislocations in silicon is substantially modified by the discreteness correction. For shuffle dislocations, the widths are broadened doubly by the discrete effect, and Peierls stresses calculated from total energy are greatly lowered. For glide dislocations, the correction for the discrete effect is relatively small, especially for 30° partial dislocation. The Peierls barrier calculated here is in the range of 0.12–0.28 eV Å^{-1} for 30° partial dislocation and 8.5–28 meV Å^{-1} for shuffle dislocations. The Peierls stress is in the range of 0.065–0.16 eV Å^{-3} for 30° partial dislocation and 3.4–8.4 meV Å^{-3} for shuffle dislocations. Apparently, the activating energy of glide and shuffle dislocations belongs to a different energy scale. The dislocations in silicon are actually divided into two categories according to their quite different Peierls barriers and stresses. As a consequence, the glide and shuffle dislocations should be respectively involved in processes with different energy scales. From careful calculation of total energy, it is found that the dislocation core may exhibit different fine structure and there is a metastable state for glide 90° and shuffle screw dislocations.

For a crystal, there may exist many kinds of dislocations, edge, screw and mixed dislocations, etc. In principle, the Burgers vectors may be distinct in both magnitude and direction. However, the fundamental question is which kind of dislocation is responsible for crystal plasticity. Some dislocations may exist in crystals, but if the activation energy is too high to be activated, they have nothing to do with the process of plastic deformation. On the other hand, some dislocations may be activated easily, but if their energy is too high to exist stably, these dislocations will decay into one with lower energy. Therefore, the dislocation responsible for crystal plasticity must be the one that has low energy and can be easily activated. For silicon, the glide and shuffle dislocations have the same Burgers vectors and so there is no obstacle preventing transformation between them. In experiment, dissociated dislocations separated by an intrinsic stacking fault are observed [10–12]. Since the stable stacking fault can exist only in the glide set, it can be concluded that glide dislocations should have lower energy. Based on the results obtained by our calculation and experimental observations, we suggest that at low temperature, shuffle dislocations are absent due to their high energy and plastic behavior being dominated by the glide dislocations. Because the glide dislocations are hardly to be moved, silicon is brittle at low temperature. At high temperature, a great number of shuffle dislocations are excited and plastic behavior is dominated by the shuffle dislocations. Because the shuffle dislocations can be moved as easily as those in BCC metals, silicon is ductile at high temperature.

Acknowledgments

The authors wish to thank Rui Wang and Jian Jiao for their helpful discussions and suggestions. The work is supported by the National Natural Science Foundation of China (grant No. 10774196) and Chongqing University Postgraduates' Science and Innovation Fund (grant No. 200904A1A0010315).

References

[1] Yonenaga I and Sumino K 1978 *Phys. Status Solidi* a **50** 685
[2] Schroter W, Brion H G and Siethoff H 1983 *J. Appl. Phys.* **54** 1816
[3] Omri M, Tete C, Michel J-P and George A 1987 *Phil. Mag.* A **55** 601
[4] Castaing J, Veyssiere P, Kubin L P and Rabier J 1981 *Phil. Mag.* A **44** 1407
[5] Kojima K and Sumino K 1971 *Cryst. Lattice Defects* **2** 147
[6] Samuels J and Roberts S G 1989 *Proc. R. Soc.* A **421** 1
[7] Hirsch P B, Roberts S G and Samuels J 1989 *Proc. R. Soc.* A **421** 25
[8] Suzuki T, Yonenaga I and Kirchner H O K 1995 *Phys. Rev. Lett.* **75** 3470
[9] Hirth J P and Lothe J 1982 *Theory of Dislocations* 2nd edn (New York: Wiley)
[10] Hirsch P B 1985 *Sci. Technol.* **1** 666
[11] Duesbery M S and Richardson G Y 1991 *Crit. Rev. Solid State Mater. Sci.* **17** 1
[12] Alexander H and Teichler H 1993 *Materials Science and Technology* vol 4, ed R W Cahn, P Hassen and E J Kramer (Cambridge: VCH Weiheim) p 249
[13] Suzuki T and Takeuchi S 1988 *Rev. Phys. Appl.* **23** 685
[14] Suzuki T and Takeuchi S 1989 *Lattice Defects in Ceramics* (*JJAP Series No. 2*) ed S Takeuchi and T Suzuki (Tokyo: Publ. Off. of Jpn. J. Appl. Phys.) p 9
[15] Duesbery M S and Joos B 1996 *Phil. Mag. Lett.* **74** 253
[16] Duesbery M S, Joos B and Michel D J 1991 *Phys. Rev.* B **43** 5143
[17] Oyama N and Ohno T 2004 *Phys. Rev. Lett.* **93** 195502
[18] Nunes R W, Bennetto J and Vanderbilt D 1998 *Phys. Rev.* B **57** 10388
[19] Nunes R W, Bennetto J and Vanderbilt D 1996 *Phys. Rev. Lett.* **77** 1516
[20] Scarle S, Ewels C P, Heggie M I and Martsinovich N 2004 *Phys. Rev.* B **69** 075209
[21] Valladares A, White J A and Sutton A P 1998 *Phys. Rev. Lett.* **81** 4903
[22] Joos B and Duesbery M S 1997 *Phys. Rev.* B **55** 11161
[23] Hansen L B, Stokbro K, Lundqvist B I, Jacobsen K W and Deaven D M 1995 *Phys. Rev. Lett.* **75** 444

[24] Pizzagalli L, Pedersen A, Arnaldsson A, Jonsson H and Beauchamp P 2008 *Phys. Rev.* B **77** 064106
[25] Miyata M and Fujiwara T 2001 *Phys. Rev.* B **63** 045206
[26] Wang C-Z, Li J, Ho K-M and Yip S 2006 *Appl. Phys. Lett.* **89** 051910
[27] Kaxiras E and Duesbery M S 1993 *Phys. Rev. Lett.* **70** 3752
[28] Ren Q, Joos B and Duesbery M S 1995 *Phys. Rev.* B **52** 13223
[29] Justo J F, de Koning M and Cai W 2000 *Phys. Rev. Lett.* **84** 2172
[30] Gomez A M and Hirsch P B 1977 *Phil. Mag.* **36** 169
[31] Wessel K and Alexander H 1977 *Phil. Mag.* A **35** 1523
[32] Hirsch P B 1980 *J. Microsc.* **118** 3
[33] Kolar H R, Spence J C H and Alexander H 1997 *Phys. Rev. Lett.* **77** 4031
[34] Joos B, Ren Q and Duesbery M S 1994 *Phys. Rev.* B **50** 5890
[35] Joos B and Duesbery M S 1997 *Phys. Rev. Lett.* **78** 266
[36] Juan Y-M and Kaxiras E 1996 *Phil. Mag.* A **74** 1367
[37] Miyata M and Fujiwara T 1998 *Meeting Abs. PSJ* **53** 99
[38] Bigger J R K *et al* 1992 *Phys. Rev. Lett.* **69** 2224
[39] Li C X, Meng Q Y, Zhong K Y and Wang C Y 2008 *Phys. Rev.* B **77** 045211
[40] Peierls R E 1940 *Proc. Phys. Soc.* **52** 23
[41] Christian J W and Vitek V 1970 *Rep. Prog. Phys.* **33** 307
[42] Bulatov V V and Kaxiras E 1997 *Phys. Rev. Lett.* **78** 4221
[43] Wang S F 2002 *Phys. Rev.* B **65** 094111
[44] Wang S F 2005 *Chin. Phys.* **14** 2575
[45] Wang S F 2009 *J. Phys. A: Math. Theor.* **42** 025208
[46] Wang S F, Liu R P and Wu X Z 2008 *J. Phys.: Condens. Matter* **20** 485207
[47] Wu X Z and Wang S F 2009 *Front. Mater. Sci. China* **3** 205
[48] Jakata K and Every A G 2008 *Phys. Rev.* B **77** 174301
[49] Maranganti R and Sharma P 2007 *Phys. Rev. Lett.* **98** 195504
Maranganti R and Sharma P 2007 *J. Mech. Phys. Solids* **55** 1823
[50] Every A G and McCurdy A K 1992 *Second and Higher Order Elastic Constants* (*Landolt-Bornstein, New Series, Group III* vol 29) (Berlin: Springer) Pt A
[51] Lejcek L 1972 *Czech. J. Phys. B.* **22** 802
[52] Kroupa F and Lejcek L 1972 *Czech. J. Phys. B.* **22** 813
[53] Wang S F 2003 *Phys. Lett.* A **313** 408
[54] Wang S F 2006 *Chin. Phys.* **15** 1301
[55] Li C X, Meng Q Y, Li G and Yang L J 2006 *Superlatt. Microstruct.* **40** 113
[56] Jing Y H, Meng Q Y and Zhao W 2009 *Physica* B **404** 2138
[57] Pizzagalli L, Godet J and Brochard S 2009 *Phys. Rev. Lett.* **103** 065505
[58] Koizumi H, Kamimura Y and Suzuki T 2000 *Phil. Mag.* A **80** 609
[59] Pizzagalli L and Beauchamp P 2004 *Phil. Mag. Lett.* **84** 729
[60] Tang Q H 2008 *Chin. Phys. Lett.* **25** 2946